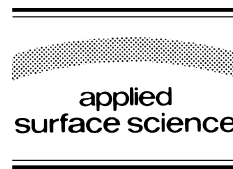




ELSEVIER

Applied Surface Science 127–129 (1998) 117–121



# Photopolymers designed for laser ablation – photochemical ablation mechanism

Thomas Lippert <sup>a,\*</sup>, J.T. Dickinson <sup>b</sup>, S.C. Langford <sup>b</sup>, H. Furutani <sup>c</sup>, H. Fukumura <sup>c</sup>,  
H. Masuhara <sup>c</sup>, T. Kunz <sup>d</sup>, A. Wokaun <sup>d</sup>

<sup>a</sup> *Los Alamos National Laboratory, MS J 585, Los Alamos, NM 87545, USA*

<sup>b</sup> *Department of Physics, Washington State University, Pullman, WA 99164-2814, USA*

<sup>c</sup> *Osaka University, Department of Applied Physics, Osaka 565, Japan*

<sup>d</sup> *Paul Scherrer Institute, Department of General Energy Research, 5232 Villigen, Switzerland*

## Abstract

We have designed photopolymers based on a photolabile chromophore with absorption properties tailored for a specific irradiation wavelength. The introduction of the two photolabile groups ( $-N=N-N<$ ) into one repetition unit of the main polymer chain results in a well-defined decomposition pathway. The exothermic decomposition mechanism yields high energetic, gaseous products, which are not contaminating the polymer surface. The products of laser ablation were studied with time-of-flight mass spectroscopy (TOF-MS). All products are totally compatible with a photochemical decomposition mechanism and their high energies can be explained by a laser induced microexplosion. Time resolved techniques, such as transmission, reflectivity or surface interferometry, revealed a ‘dynamic’ behavior. Ns-interferometry showed that etching of the polymer nearly starts and ends with the laser pulse. During the initial stages of the irradiation, darkening of the surface was detected, which corresponds to a decrease of reflectivity and an increase of transmission. This is due to a decrease of the refractive index and absorption coefficient, caused by the photodecomposition of the polymer starting with the irradiation pulse. © 1998 Elsevier Science B.V.

PACS: 81.60; 42.10; 82.50

Keywords: Photopolymer; Laser ablation; Mechanism; Excimer laser; Triazenopolymer

## 1. Introduction

Rapid prototyping with high spatial resolution impacts a number of technologies including applications of photolithography to production of semiconductor circuitry, sensors, and micromechanical devices. Laser ablation is a powerful technique for

rapid patterning of very small features which can be applied for a number of different materials [1]. In comparison with conventional photolithography, laser ablation has several advantages. The most important of them is the fact that this is a dry etching process with a smaller number of processing steps [2]. The shortcomings usually associated with laser patterning, such as the low efficiency of the ‘expensive’ laser photons and thermal effects leading to the re-deposition of ablation products, are mainly related

\* Corresponding author. Tel.: +1-505-665-4379; fax: +1-505-665-4817; e-mail: lippert@lanl.gov.

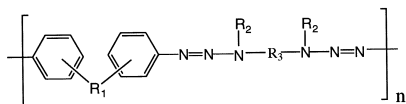


Fig. 1. Structural unit of the triazenopolymers.

to the use of standard polymers which have been designed for totally different purposes.

Our specially designed photopolymers are based on a photolabile chromophore with absorption properties tailored for a specific irradiation wavelength (e.g., 308 nm XeCl laser). The structural formula is shown in Fig. 1. By varying the substituents  $R_1$  to  $R_3$ , the properties of the polymers can be changed in a wide range, as shown in Table 1.

With the incorporation of photolabile groups into the main chain of the polymer, we expected to overcome several of the aforementioned shortcomings of laser ablation: (a) the defined decomposition pathway should result in gaseous products (no surface contamination) and no surface modifications (changing etch rate and quality); (b) a photochemical mechanism has an intrinsically higher resolution (no thermal damages).

The mechanism of polymer laser ablation is still a controversial topic. For most polymers, especially at wavelengths longer than 193 nm, a photothermal mechanism is favored by many research groups [5]. With the use of a well-defined photolabile system, we hoped to 'shift' the mechanism to a decomposition pathway dominated by photochemical features. Here we report results from a combination of various analytical techniques to study the ablation mechanism.

Table 1  
Physico-chemical properties of the triazenopolymers [3,4]

$\lambda_{\max}^a$	293–381 nm
QY <sup>b</sup>	0.12–0.74%
$T_{\text{dec}}^c$	221–300°C
$T_G^d$	33–110°C

<sup>a</sup>Absorption maximum measured in THF.

<sup>b</sup>Quantum yield of photodecomposition in THF with 308-nm irradiation.

<sup>c</sup>Decomposition temperature, measured with DSC.

<sup>d</sup>Glass transition temperature, measured with DSC.

## 2. Experimental setup

The polymers were synthesized by an interfacial polycondensation as reported elsewhere [3,4]. Due to the different laser equipment for the various experimental set-ups two different polymers have been used. For both polymers  $R_2 = \text{CH}_3$  and  $R_3 = \text{C}_6\text{H}_{12}$ . For the ns-transmission, reflectivity and interferometry experiments  $R_1 = m\text{-SO}_2$  and the irradiation source was a XeF (351 nm) excimer laser. For all other experiments, a polymer with  $R_1 = p\text{-O}$  and a XeCl (308 nm) or KrF (248 nm), excimer laser have been used. Both the 308- and 351-nm irradiation are close to the absorption maximum of the polymers, and result in an excitation of the  $\pi\text{-}\pi^*$  transition of the triazene group [6]. The experimental set-up for the transmission and reflectivity experiments [7], ns-interferometry [8,9] and TOF-MS [10] have been reported previously.

## 3. Results and discussion

To determine the ablation mechanism, we initially compared the etching quality between the triazenopolymer (TP) and polyimide (PI). Both polymers have similar linear absorption coefficients ( $\alpha_{\text{lin}}$ ) and for PI, a photothermal ablation mechanism has

Table 2  
Comparison of the ablation parameter at 308 nm for PI and TP

	Polyimide	Triazenopolymer
$\alpha_{\text{lin}}^a$	$1.0 \times 10^5 \text{ cm}^{-1}$ [12]	$1.66 \times 10^5 \text{ cm}^{-1}$ [13]
$\alpha_{\text{eff}}^b$	$0.9 \times 10^5 \text{ cm}^{-1}$ [12]	$0.18 \times 10^5 \text{ cm}^{-1}$ [13]
$d_{\max}/\text{pulse}^c$	$\sim 1.5 \mu\text{m}$	$\sim 3.2 \mu\text{m}$ [13]
Surface modification <sup>d</sup>	yes, carbonization [14]	no [15,16]
Product re-deposition <sup>e</sup>	yes [17]	no [13,15,16]

<sup>a</sup>Linear absorption coefficient.

<sup>b</sup>Effective absorption coefficient, measured from the slope of the etch rate vs. fluence, according to  $d(F) = \alpha_{\text{eff}}^{-1} \ln(F/F_0)$ , where  $F$  = laser fluence and  $F_0$  = threshold fluence.

<sup>c</sup>Maximum etch rate per pulse, for a fluence  $\sim 20 \text{ J cm}^{-2}$ .

<sup>d</sup>Measured after irradiation with surface sensitive techniques.

<sup>e</sup>Controlled by scanning electron microscopy and other analytical techniques.

been established for irradiation at 308 nm [11]. In Table 2, several parameters of ablation at 308 nm for PI and TP are compared.

Both polymers have linear absorption coefficients ( $\alpha_{\text{lin}}$ ) in a similar range, but the high fluence or effective absorption coefficient ( $\alpha_{\text{eff}}$ ) are quite different. For PI, there is hardly any difference between the linear and effective absorption coefficient, whereas  $\alpha_{\text{eff}}$  of TP is one order of magnitude lower than  $\alpha_{\text{lin}}$ , causing the higher  $d_{\text{max}}$  of TP. The absence of surface modifications and debris on the polymer surface after ablation of TP suggests a possible application in a ‘real’ one-step dry etching process; it does not require additional cleaning steps. The differences in the etching quality between PI and TP are shown in Fig. 2. The microstructure etched into PI reveals damages most likely due to thermal effects, whereas the microstructure in TP is much better defined. (This allowed the use of an atomic force microscope, AFM, for measuring the microstructure, whereas the structure in PI was too rough to use the AFM.)

To study the ablation mechanism in a more detailed manner, time resolved techniques such as ns-reflectivity, transmission and surface interferometry, were combined with data from an ablation product

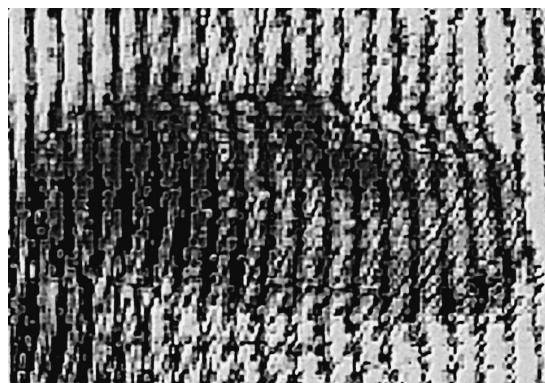


Fig. 3. Interferometric images after irradiation with  $250 \text{ mJ cm}^{-2}$ ; time.

sensitive technique (TOF-MS). Ns-surface interferometry is a powerful tool to probe the surface morphology during laser irradiation. One example of a surface interference pattern is shown in Fig. 3. In this image, taken 8 ns after the laser pulse maximum, two important features can be recognized: darkening of the polymer surface in the area of the laser beam and slight shift of the interference fringes to the right, which corresponds in this configuration to an etching of the polymer. An analysis of several fringe

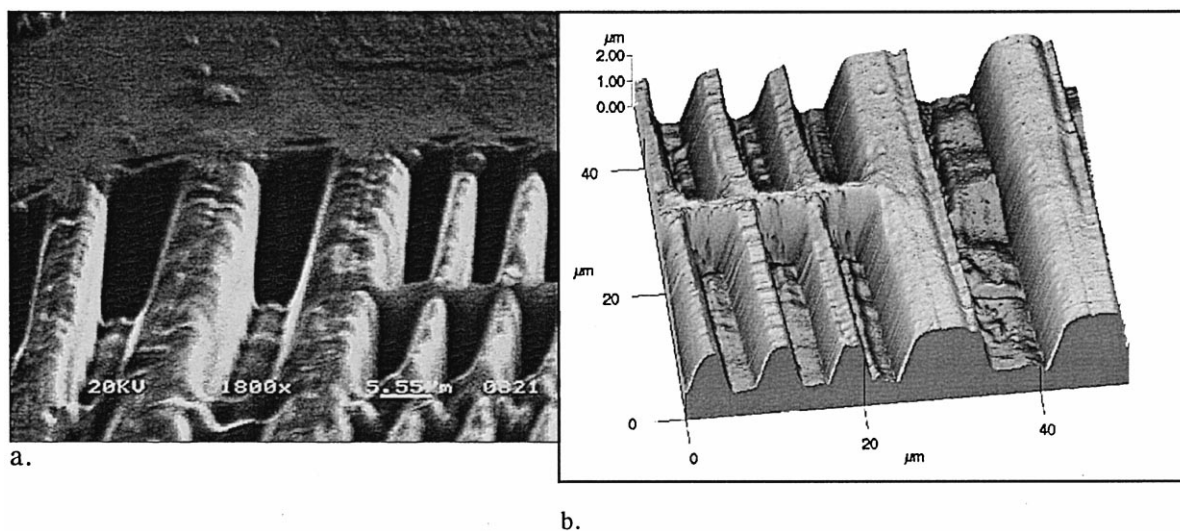


Fig. 2. SEM picture of PI, 12 pulse  $9.3 \text{ J cm}^{-2}$  (a). AFM picture of ablated triazenopolymer; 1 pulse: fluence  $7.5 \text{ J cm}^{-2}$  (b).

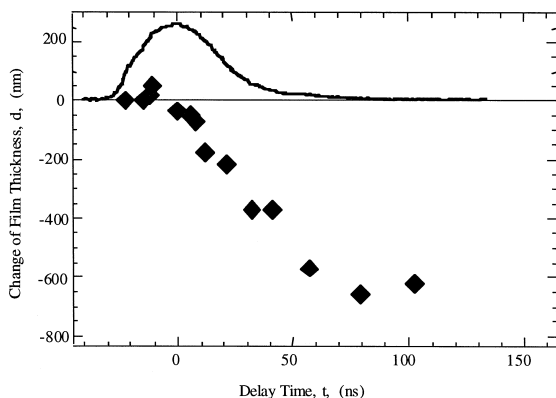


Fig. 4. Time resolved etching of the polymer with a fluence of  $250 \text{ mJ cm}^{-2}$ . The curve is the integration of the laser pulse.

shifts (Fig. 4) shows that etching of the polymer nearly starts and ends with the laser pulse at this fluence (at lower fluences a deviation of this behavior has been found [7]) (Fig. 5). This is a strong indication for a photochemical mechanism, because for photothermal systems surface swelling and a time delayed etching always has been observed [8,18]. The darkening of the polymer surface in the irradiated area was studied in more detail with both time resolved reflectivity and transmission measurements at a wavelength (580 nm) where the polymer has a very low absorption. The results are shown in Fig. 5. The reflectivity of the polymer film decreased simultaneously with the observed darkening of the surface, whereas an increase of the transmission followed by

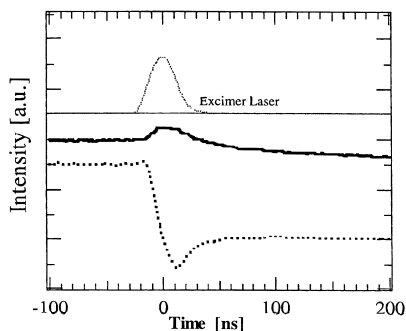


Fig. 5. Time resolved reflectivity and transmission of the triazenopolymer. The dotted curve represents the reflectivity.

a decrease can be observed. The decrease of the transmission starting after the end of the laser pulse can be assigned to the attenuation of the probe beam by the ejected products. The change of the reflectivity and transmission in opposite directions clearly shows that microbubbles or surface roughening are not the reason for the observed darkening. Reversible melting during a photothermal process usually leads to an increase of reflectivity. Therefore, we suggest that the photochemical decomposition causes a decrease of the refractive index and absorption coefficient. This is supported by a previous study [6] where a transmission increase of the laser pulse through thin films.

For additional data on the ablation mechanism, the decomposition products were studied using TOF mass spectroscopy. The main products of ablation are low molecular weight neutral fragments, shown in Fig. 6. Ionic species were only detected after irradiation with fluences above  $1.3 \text{ J cm}^{-2}$  and could be assigned to  $\text{C}_2^+$  or  $\text{CN}^+$  species. The detected neutral fragments are totally compatible with the photochemical decomposition mechanism previously reported for aryl-dialkyl-triazeno compounds [19]. The first step in the decomposition is the homolytic bond scission between the N–N bond, followed by the extrusion of the main fragment,  $\text{N}_2$ , from the unstable diazo-radical. Both other fragments (bis-

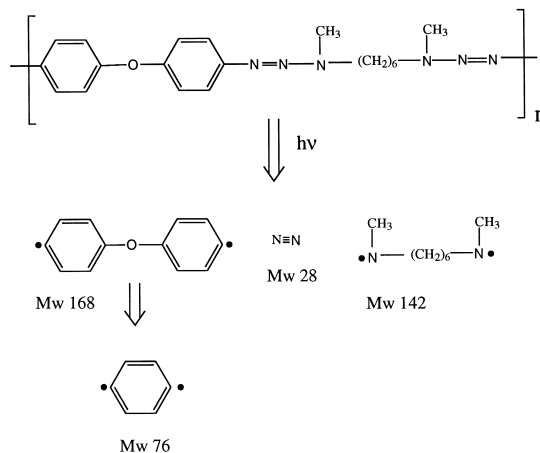


Fig. 6. Fragments found in the TOF-MS of the triazenopolymer after irradiation at 248 nm. The position of the radicals is only used to improve the understanding of the mechanism, in detail, the homolytic bond scission.

phenyl ether and bis-amino species) of the primary decomposition step were detected also. Due to the irradiation wavelength (248 nm) in these experiments, the phenyl species were another main fragment. This is most probably due to absorption of the laser wavelength by the bis-phenyl ether species, which results in further decomposition. Analyzing the TOF curves revealed high energetic particles which are not compatible with a thermal decomposition mechanism, but rather an explosive process. A similar result has been derived from a previous study of shock waves after laser irradiation of TP. The speed of the shock waves could be described by a model describing the process as a laser induced microexplosion [20].

#### 4. Conclusion

The application of specially designed photolabile polymers for laser ablation results in a dry etching process with no additional cleaning steps. The ablation mechanism is mainly photochemical at the applied laser fluences. The etching of the polymer starts and ends with the laser pulse and the decomposition of the polymer can be detected even before etching takes place. The ablation products are totally compatible with the photochemical decomposition and the energies calculated from the time of flight curves are not in the range of a thermal mechanism.

#### Acknowledgements

T.L. expresses his gratitude to Los Alamos National Laboratory for research fellowships.

#### References

- [1] K. Jain, *Excimer Laser Lithography*, SPIE, The International Society for Optical Engineering, Bellingham, 1990.
- [2] K. Suzuki, M. Matsuda, T. Ogino, N. Hayashi, T. Terabayashi, K. Amemiya, *Proc. SPIE* 2992 (1997) 98.
- [3] J. Stebani, O. Nuyken, T. Lippert, A. Wokaun, *Makromol. Chem. Rapid Commun.* 206 (1993) 97.
- [4] J. Stebani, O. Nuyken, T. Lippert, A. Wokaun, A. Stasko, *Makromol. Chem. Phys.* 196 (1995) 739.
- [5] G.C. D' Couto, S.V. Babu, *J. Appl. Phys.* 76 (1994) 3052.
- [6] T. Lippert, L.S. Bennett, T. Nakamura, H. Niino, A. Ouchi, A. Yabe, *Appl. Phys. A* 63 (1996) 257.
- [7] H. Furutani, H. Fukumura, H. Masuhara, T. Lippert, A. Yabe, *J. Phys. Chem.* (1997), in press.
- [8] H. Furutani, H. Fukumura, H. Masuhara, *Appl. Phys. Lett.* 65 (1994) 3413.
- [9] T. Lippert, L.S. Bennett, T. Kunz, C. Hahn, A. Wokaun, H. Furutani, H. Fukumura, H. Masuhara, T. Nakamura, A. Yabe, *Proc. SPIE* 2992 (1997) 135.
- [10] R.L. Webb, S.C. Langford, J.T. Dickinson, *Nucl. Instr. Meth. B* 103 (1995) 297.
- [11] S. Küper, J. Brannon, K. Brannon, *Appl. Phys. A* 56 (1993) 43.
- [12] J.H. Brannon, J.R. Lankard, A.I. Baise, F. Burns, J. Kaufman, *J. Appl. Phys.* 58 (1985) 2036.
- [13] T. Lippert, J. Stebani, J. Ihlemann, O. Nuyken, A. Wokaun, *J. Phys. Chem.* 97 (1993) 12296.
- [14] X.J. Gu, *Appl. Phys. Lett.* 62 (1993) 1568.
- [15] T. Lippert, L.S. Bennett, T. Nakamura, H. Niino, A. Yabe, *Appl. Surf. Sci.* 96–98 (1996) 601.
- [16] T. Lippert, T. Nakamura, H. Niino, A. Yabe, *Macromolecules* 29 (1996) 6301.
- [17] G. Koren, J. Donelon, *J. Appl. Phys. B* 45 (1988) 45.
- [18] H. Furutani, H. Fukumura, H. Masuhara, *J. Phys. Chem.* 100 (1996) 6871.
- [19] T. Lippert, J. Stebani, A. Stasko, O. Nuyken, A. Wokaun, *J. Photochem. Photobiol.* 78 (1994) 139.
- [20] L.S. Bennett, T. Lippert, H. Furutani, H. Fukumura, H. Masuhara, *Appl. Phys. A* 63 (1996) 327.